The influences of loading path and end friction on the stress distributions in a bi-axially compressed specimen in two-dimensions

By Koji NAKAGAWA*

Abstract

In this paper, the influences of loading path and end friction on the stress distributions in a bi-axially compressed specimen in two-dimensions were analyzed.

In multi-axial compression tests, the effect of end friction on the stress distribution is so large, that it is desirable to apply a lubricant to the contact surfaces between the platens and the specimen. The analytical results indicate numerous suggestions which might be useful in multiaxial compression tests with steel platens.

In numerical analysis, the finite element method was employed.

1. Introduction

In order to understand the mechanical properties of rock-like materials, it is desirable that the specimen of the material be tested in a homogeneous stress or strain state. For this purpose, numerous loading devices have been employed by many investigators. In a test of rock-like materials in which steel platens are used, it must be remembered that the deformation of the specimen is disturbed by the friction at the end surfaces of the specimen, which hereafter will be called the end friction. In an ordinary uniaxial compression test, to a certain extent this friction would prevent the specimen from expanding laterally. In a multi-axial compression test with steel platens, in addition to the occurence of the above-mentioned stress disturbance, a peripheral portion of the load on the platen may be transmited to an opposite platen through the other pairs of platens. This situation makes the actual pressure in the specimen different from the apparent pressure given by the load divided by the cross sectional area of the specimen. When the ratio of the two loads on the different pairs of platens is extremely large, the specimen assumes a state of partial loading owing to its bulging.

The stress distributions in a uniaxially compressed specimen with a finite coefficient of end friction have been analysed by Niwa et. al..[1)]

Numerical data of the stress distributions in multi-axially compressed specimens, however, are not available at present. In a multi-axial compression test, we usually have to apply a lubricating material to the contact surfaces

* Department of Civil Engineering

between the platens and the specimen, although the effect of lubrication on the stress distribution in the specimen is not well understood.

In this paper, analyses of the effects of the displacement path of the loading platen and also of the coefficient of end friction on the stress distribution in the specimen are presented. This is for the purpose of obtaining data to be used in further investigations of the end effects in the multi-axial compression test of rock-like materials.

2. Presentation of problems

A two-dimensional square, elastic specimen ($2a \times 2a$) which is bi-axially compressed between two pairs of parallel rigid platens is analyzed (Fig. 1).

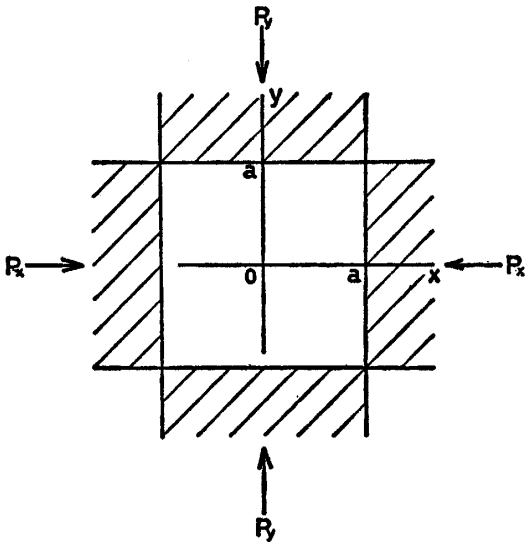

Fig. 1 Two-dimensional specimen and two-dimensional coordinate axes

It is assumed that throughout the process of loading, the specimen is elastic and in the state of plane strain and isotropically homogeneous. In an ordinary multi-axial compression test with steel platens, the specimen is in the state of partial loading, owing to the fact that, in an experimental procedure, the cross section of the loading platen is made actually a little smaller than that of the specimen in order to avoid contact between adjacent platens. However, in an analytical calculation of this test, the cross section of the loading platen is assumed to be equal to that of the specimen.

In an ordinary compression test with steel platens, the load control method or the platen displacement control method is employed. The load control method has the disadvantage of rendering the analytical calculation difficult, and thus in this work, the platen displacement control method was employed.

2–1. The displacement paths of loading platens

In uniaxial compression tests, we have only one displacement path which

reaches a certain greatest displacement. Therefore, the stress distribution in the specimen is determined uniquely by the platen displacement. In a bi-axial compression test, however, there are an infinite number of platen displacement paths for a certain greatest value of the palten displacement. Along each platen displacement path in the bi-axial compression test, the frictional force on the specimen end acts independently. The stress distribution in the specimen is different for different platen displacement paths, even if the elastic moduli of the specimen, the platen conditon and the coefficient of end friction are taken to be constant.

As an example, let us take a platen displacement path in which the side (x-direction, Fig. 1) displacement takes place after the axial (y-direction) one has been fixed at its final value. The specimen which has bulged due to the axial compression is then compressed by another pair of platens. At first, each of the x-axis platens makes contact with the specimen side at one point. The contact surface increases gradually as the displacement of side platen increases, and eventually the surface contact becomes total (Fig. 2).

As another example, let us take the path in which, after an isotropic com-

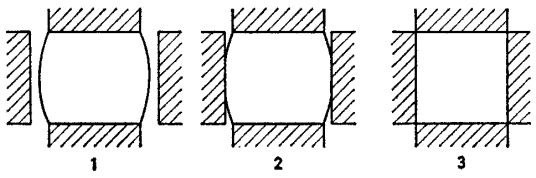

Fig. 2 Loading process and deformation of the specimen (uniaxial compression → isotropic compression)

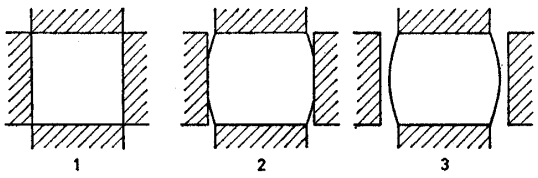

Fig. 3 Loading process and deformation of the specimen (isotropic compression → uniaxial compression)

pression, the platen displacement δ_y is increased while simultaneously δ_x is decreased (Fig. 3). Owing to the constraint by the frictional force at the specimen end, the side displacement (x-direction) of the specimen produces such a bulge, that the contact surface with the side platen takes place only in the central part of the specimen side and eventually this contact surface decreases to a point (Fig. 3).

In this study, only three of the infinite number of the platen displacement paths are analysed as typical examples. These three are the two platen displacement paths mentioned above (cases A and C, Fig. 4) and one in which the two platen displacements are proportional to each other (case B, Fig. 4), which will be called the proportional platen displacement.

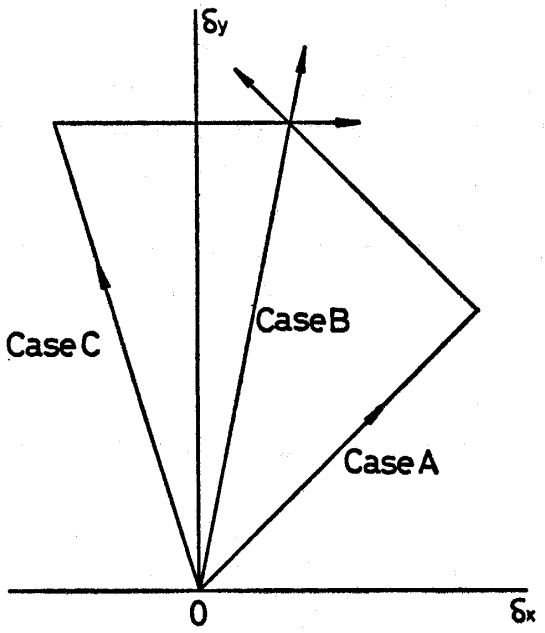

Fig. 4 Examples of loading paths

2–2. Processes of numerical analysis depending on the platen displacement path

In the present simulation analysis, it is necessary to assume several different conditions which are to be employed in succession. The following simulating processes were employed for the case of each of the platen displacement paths:
1) Case A: The platen displacement δ_y increases and then δ_x simultaneously decreases, after an isotropic compression.

After δ_y and δ_x have attained certain equal values, under fixed end conditions, the constraints at the contact surfaces are gradually released until a certain finite coefficient of friction is obtained. Then, in the next procedure, a small increase $\Delta\delta_y$ in δ_y and a small decrease $-\Delta\delta_x$ in δ_x, where $\Delta\delta_y=\Delta\delta_x$, are added to the initial values of δ_y and δ_x respectively. This procedure is continued until certain predetermined values of the platen displacements are attained.

2) Case B: Proportional platen displacement

At first, the platen displacements are given with perfect end constraint, and then the constraints are released gradually until a certain finite coefficient of end friction is obtained.

3) Case C: After the uniaxial compression, the side platen displacement is increased.

The specimen is compressed uniaxially in y-direction with a certain coefficient of end friction (uniaxial compression state). Then the side platen displacement δ_x is increased until a certain platen displacement condition is reached.

2–3. End constraint and coefficient of end friction

The end constraint of the specimen with the rigid loading platen is controlled by the coefficient of friction between them. The coefficient of friction in statical mechanics is assumed. Strictly speaking, the coefficient of friction may vary as the axial load increases and the initial irregularities of the end surface are gradually smoothed out. In the present study, the coefficient of friction is assumed to be constant irrespective of the magnitude of the normal stress for the sake of simplicity.

In uniaxial compression tests, the compression state of the specimen with a fixed end is an example of a compression test which simulates the uniaxial compression test without lubricating materials. However, in bi-axial compression test, the load is not transmitted through the specimen which is fixed to the rigid platens. The load applied to the platen is transmitted to the opposite platen only through the perpendicular pairs of platens. Therefore, it is meanigless to discuss the stress distribution in the specimen with fixed end subject to bi-axial compression.

2–4. Numerical analysis

In the numerical analysis, the finite element method was employed.

3. Numerical results and discussion

For the numerical analysis, concrete was chosen as the model material and Poisson's ratio was assumed to be $\nu=1/6$. The effects of platen displacement paths (for the three cases) and the coefficients of end friction ($\mu=0.2$, 0.1 and 0.05) on the stress distributions in the specimen were analyzed. In following discussion the stresses are made dimensionless by dividing their values by the average stress in the y-direction σ_{y0}.

3–1. The effect of the platen displacement path on the stress distributions in a bi-axially compressed specimen

The effect of the platen displacement path on the stress distributions in the specimen will be discussed. The coefficient of end friction is assumed to be $\mu=0.2$.

(a) Stress distribution in the specimen

The distributions of σ_y in cases A and C with $\delta_x/\delta_y=1.0$ are shown in Fig. 5. With $\delta_x/\delta_y=1.0$ (apparent isotropic compression state), the loading condition in case A coincides with that in case B. In case A, a considerable portion of the load in the y-direction cannot reach the central section of the specimen ($y=0$) because of the frictional constraint at $x=a$. The decrease in σ_y is extremely large near the end $x=a$ at the central section ($y=0$). At the corner, σ_y becomes very large. In case C, the deviation of σ_y from the average value is smaller than that in case A. With $\delta_x/\delta_y=0.1$ and -0.1, similar but smaller deviations of σ_y from the average values are seen than in the case for which

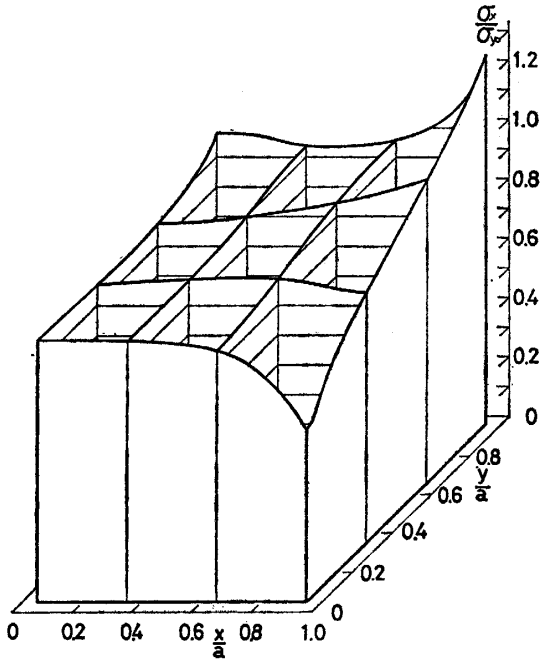

Fig. 5–1 Distribution of σ_y/σ_{y0}
case A, $\mu=0.2$, $\delta_x/\delta_y=1.0$
(σ_{y0}: apparent stress in y-direction)

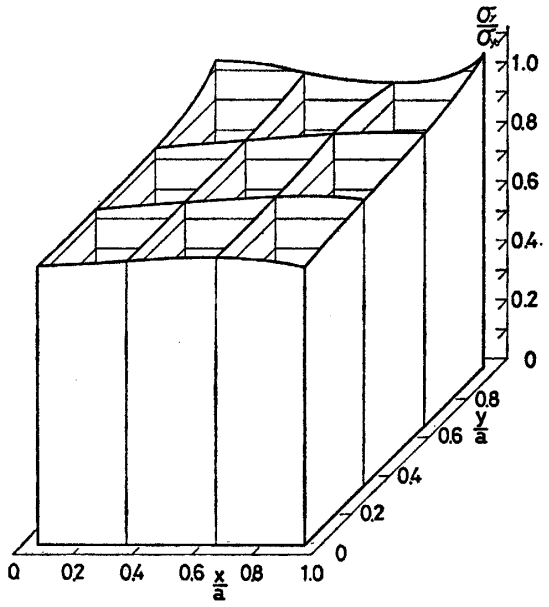

Fig. 5–2 Distribution of σ_y/σ_{y0}
case C, $\mu=0.2$, $\delta_x/\delta_y=1.0$
(σ_{y0}: apparent stress in y-direction)

$\delta_x/\delta_y=1.0$. These distributions are explained as the result of the effect of the end friction at $x=a$. In case A, the platen in the y-direction moves against the end friction at $x=a$, while in case C, the platen in y-direction moves without frictional constraint at $x=a$.

The distributions of σ_x are shown in Figs. 6 and 7 with $\delta_x/\delta_y=0.1$ and -0.1. The effect of end friction on the distribution of σ_x in case A is larger than that in case C. With $\delta_x/\delta_y=-0.1$, the specimen is loaded partially in the x-direction as shown in Figs. 2 and 3. σ_x must be zero at the free end where

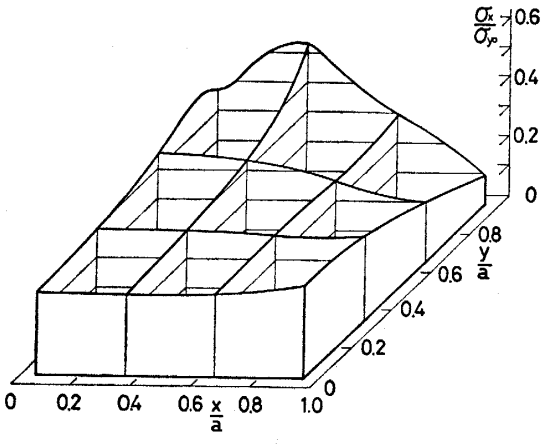

Fig. 6–1 Distribution of σ_x/σ_{y0}
case A, $\mu=0.2$, $\delta_x/\delta_y=0.1$
(σ_{y0}: apparentstress in y-direction)

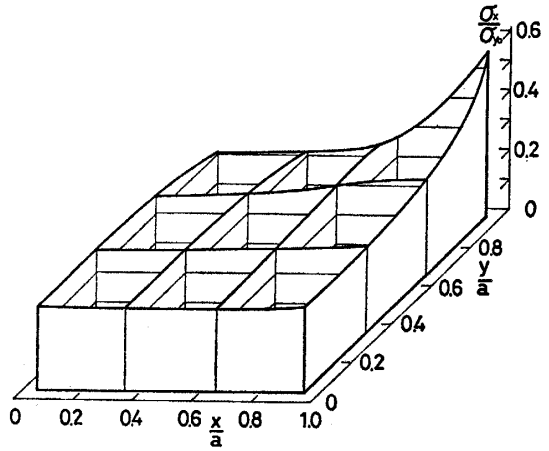

Fig. 6–2 Distribution of σ_x/σ_{y0}
case C, $\mu=0.2$, $\delta_x/\delta_y=0.1$
(σ_{y0}: apparent stress in y-direction)

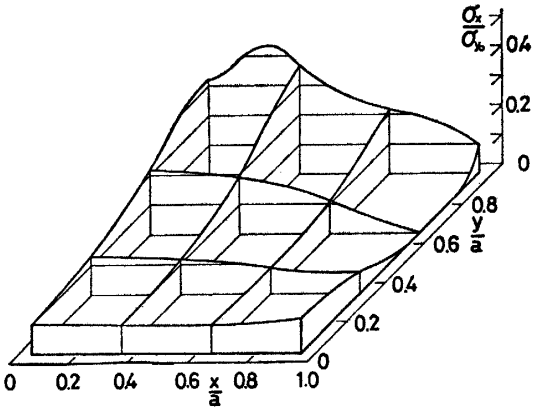

Fig. 7–1 Distribution of σ_x/σ_{y0}
case A, $\mu=0.2$, $\delta_x/\delta_y=-0.1$
(σ_{y0}: apparent stress in y-direction)

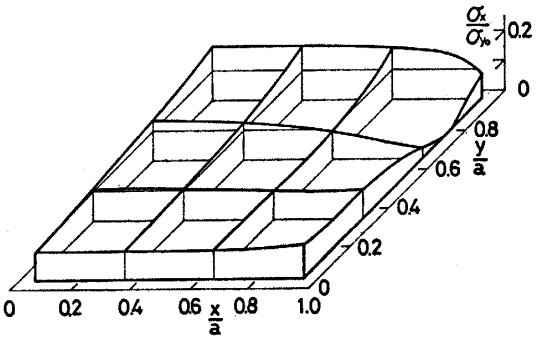

Fig. 7–2 Distribution of σ_x/σ_{y0}
case C, $\mu=0.2$, $\delta_x/\delta_y=-0.1$
(σ_{y0}: apparent stress in y-direction)

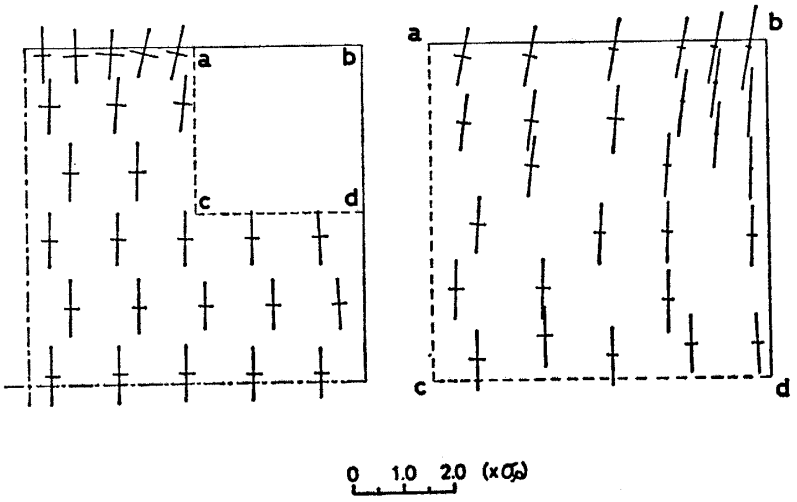

Fig. 8–1 Principal stresses and their directions
case A, $\delta_x/\delta_y=0.1$, $\mu=0.2$

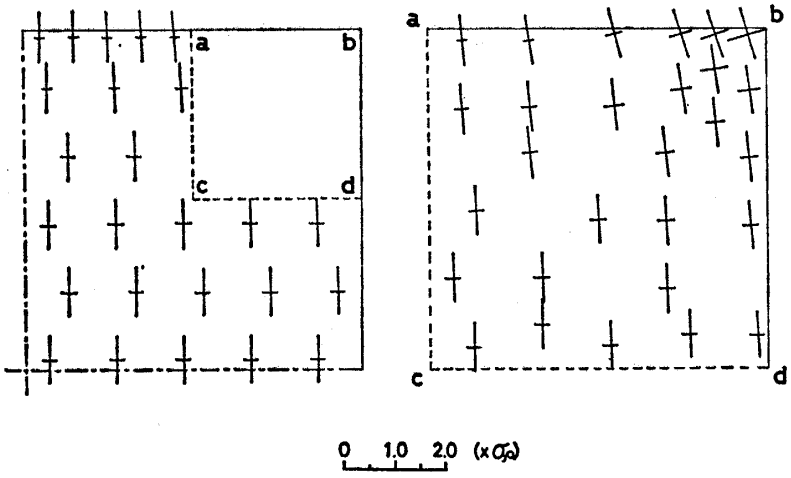

Fig. 8–2 Principal stresses and their directions
case C, $\delta_x/\delta_y=0.1$, $\mu=0.2$

the specimen does not come in contact with the platen. In Fig. 7, however, a considerable large value of σ_x exists near the corner of the figure. This is because the corner of the figure does not coincide with the corner of the specimen (stresses are calculated within the element).

In Fig. 8, the principal stresses and their directions are shown for cases A and C with $\delta_x/\delta_y=0.1$. In case A, the maximum stress runs from the end $y=a$ towards the central part (near the point $x=y=0$) of the specimen. On the other hand, in case C, it runs from the end $y=a$ towards the outer part (near the point $x=a, y=0$) of the specimen. The direction of this stress flow is generally determined by whether the x-direction displacement of the specimen in the most recent loading process is positive or negative, and it influences the distribution of σ_x and σ_y.

(b) Distributions of σ_y and τ_{yx}

σ_y and τ_{yx} at $y=a$ and σ_y at $y=0$ are shown in Fig. 9. Here, the stresses were calculated from the nodal forces. With $\delta_x/\delta_y=1.0$, the deviation of σ_y from the average value is large in case A (=case B for this displacement) and is small in case C as is shown in Fig. 5. At this platen displacement, the magnitude of τ_{yx} at $y=a$ is almost equal to μ times σ_y. This means that the frictional forces at the specimen ends try to prevent the mutual pairs of loading platens from coming together with their possible maximum magnitude. With $\delta_x/\delta_y=0.4$, τ_{yx} at $y=a$ differs from that with $\delta_x/\delta_y=1.0$. In case A, it tries to prevent the specimen from expanding in the x-direction, while in case C, it tries to prevent the specimen from shrinking in the x-direction. With $\delta_x/\delta_y=0.0$, the magni-

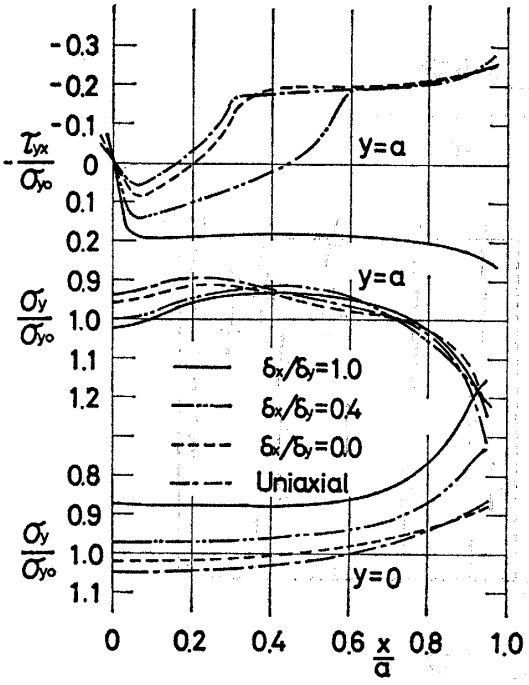

Fig. 9–1 Distributions of τ_{yx}/σ_{y0} and σ_y/σ_{y0} case A, $\mu=0.2$

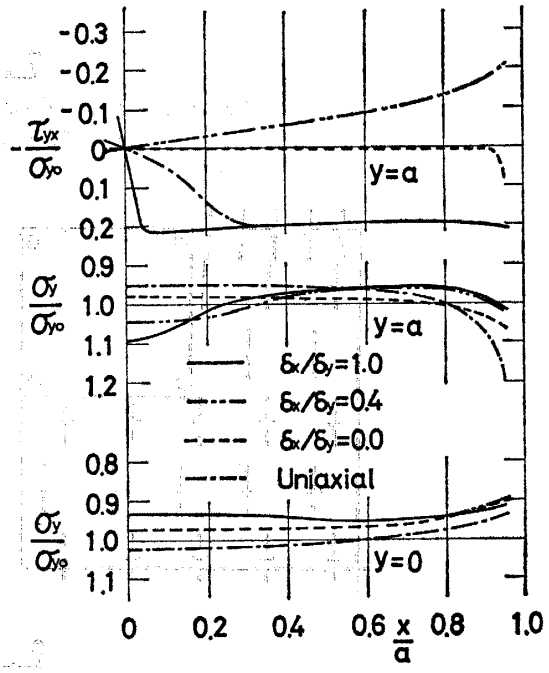

Fig. 9–2 Distributions of τ_{yx}/σ_{y0} and σ_y/σ_{y0} case C, $\mu=0.2$

tude of τ_{yx} at $y=a$ is similar to that with $\delta_x/\delta_y=0.4$ in case A, and is almost zero in case C. This zero distribution of τ_{yx} can be explained as follows. When a plane strain specimen with $\nu=1/6$ is compressed uniaxially between rigid platens with $\mu=0.2$, only a small part of the specimen end slides against the frictional force. This means that the deformation of the specimen is in almost the same state as that of the fixed end one. In case C, the platen displacement in the x-direction follows that in the y-direction, and the deformation of the speciment with $\delta_x=0$ is almost the same as a uniform deformation. This means that τ_{yx} at $y=a$ is nearly zero. For compression without an x-directional load, τ_{yx} at $y=a$ prevents the specimen from expanding in the x-direction and its magnitude in case A is larger than that in case C. From these figures the distributions of σ_y at $y=a$ and $y=0$ in cases A and C, which were discussed in a preceding article, are easily understood.

(c) Distribution of σ_x

The non-uniformities of σ_x which result from the platen displacement paths are discussed here. The stresses were calculated from the nodal forces.

The distributions of σ_x at $x=a$ and $x=0$ are shown in Fig. 10. The distributions of σ_x for several platen displacements δ_x are shown in each figure. At the center of the specimen ($x=0$, Fig. 10–1), the distributions of σ_x in case B resemble those in case C. Especially for a small platen displacement δ_x, the σ_x distributions in both cases are almost the same. In cases B and C, this figure shows that the direction of frictional force at $y=a$ is same as that of the x-direction load for $\delta_x/\delta_y<0$ and that it is oposite for $\delta_x/\delta_y>0$.

In case A, the magnitude of σ_x at the corner generally increases as y increases and decreases suddenly near $y=a$. This distribution pattern of σ_x comes from that in the unloading process the mutual displacement of the platen and the specimen end at $y=a$ is very little, especially neart he central section ($x=0$). Therefore, the stress state with $\delta_x/\delta_y=1.0$ is nearly conserved throughout the

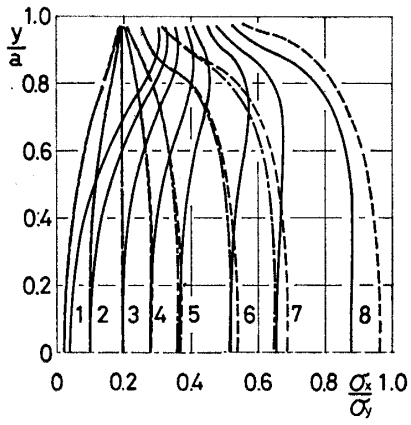

Fig. 10–1 Distributions of σ_x/σ_{y0} at $x=0$, $\mu=0.2$

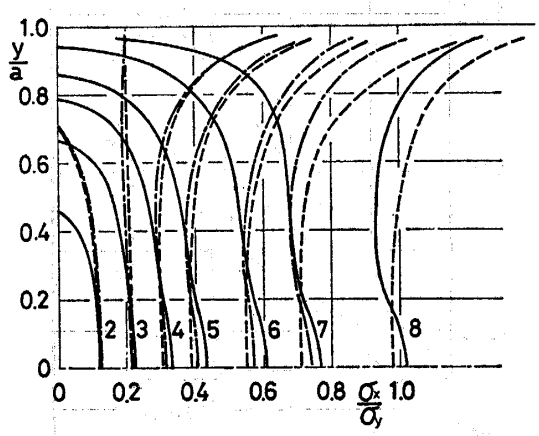

Fig. 10–2 Distributions of σ_x/σ_{y0} at $x=a$, $\mu=0.2$

—— case A, —·— case B, – – – case C

1: uniaxial, 2: $\delta_x/\delta_y=-0.1$, 3: $\delta_x/\delta_y=0$, 4: $\delta_x/\delta_y=0.1$

5: $\delta_x/\delta_y=0.2$, 6: $\delta_x/\delta_y=0.4$, 7: $\delta_x/\delta_y=0.6$, 8: $\delta_x/\delta_y=1.0$

unloading process.

For large δ_x/δ_y, the distribution of σ_x at $x=a$ in case B resembles that in case C. In case A, σ_x at the corner of the specimen is large with $\delta_x/\delta_y=1.0$, but it decreases with a decrease of the platen displacement in the x-direction. This rapid decrease of σ_x with a decrease of the platen displacement is due to insufficient deformation of the specimen which is caused by the frictional force at $y=a$. It is seen that the specimen is in a partial loading state with $\delta_x/\delta_y=0.6$.

3-2. The effect of the coefficient of friction on the stress distributions in biaxially compressed specimens

(a) Distributions of σ_y and τ_{yx}

The distributions of σ_y and τ_{yx} at $y=a$ and $y=0$ were shown in Fig. 9. Their distributions under other conditions are not shown in the figure because the distribution curves are similar in each case with $\mu=0.2$. The deviations of these values from the averages are nearly proprtional to the coefficient of end friction μ.

It is necessary to know the average value of σ_y for a fixed loading condition. In order to know these values, loads in the y-direction for a unit displacement of the lading platen under each condition are shown in Fig. 11. Here, the magnitude is made dimensionless by dividing the value by the uniaxial compression load in a perfectly lubricated specimen.

For the perfectly lubricated end condition, the specimen makes contact with the platen in the x-direction with $\delta_x/\delta_y=-0.2$. For a finite end friction, the end displacement of the specimen in the x-direction becomes rather small.

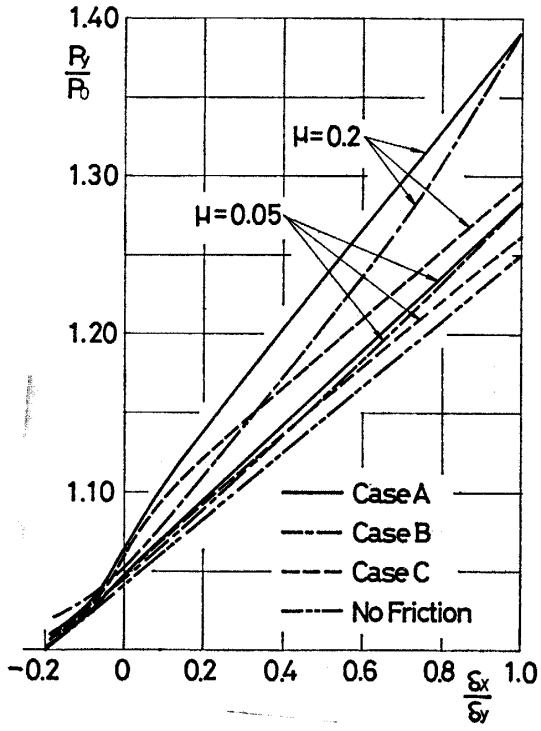

Fig. 11 *Py/Po* with various loading paths, δ_x, μ (δ_y: const. *Po*: uniaxial load necessary to realize δ_y in perfectly lubricated specimen)

Along each path, loads in the y-direction are considerably larger than in the case of a perfectly lubricated spcimen. The distribution curves are similar for each path, and deviations of the load from the load in the case of a perfectly lubricated specimen can be estimated to be proportional to the coefficient of end friction.

(b) Distribution of σ_x

In Figs. 12 and 13, the distributions of σ_x at $x=a$ and $x=0$ are shown for

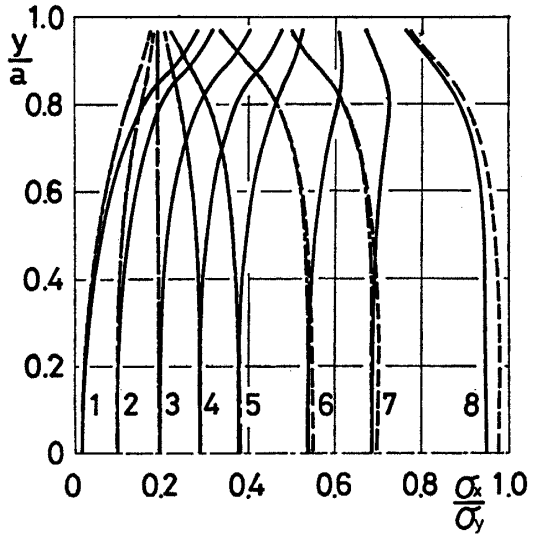

Fig. 12–1 Distributions of σ_x/σ_{y0} at $x=0$ for $\mu=0.1$

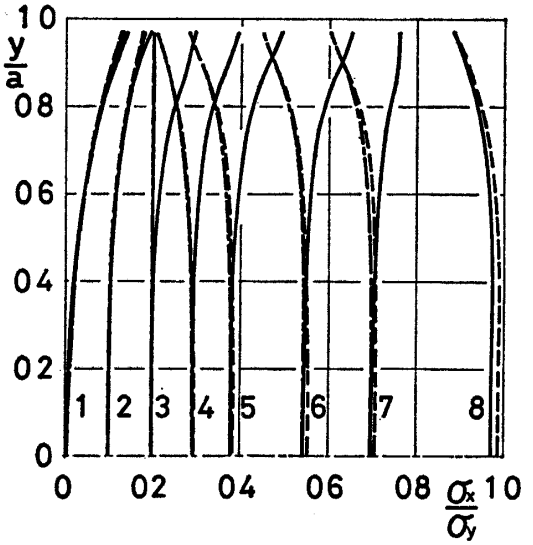

Fig. 12–2 Distributions of σ_x/σ_{y0} at $x=a$ for $\mu=0.05$

—— case A, —·— case B, —··— case C

1: uniaxial, 2: $\delta_x/\delta_y=-0.1$, 3: $\delta_x/\delta_y=0$, 4: $\delta_x/\delta_y=0.1$

5: $\delta_x/\delta_y=0.2$, 6: $\delta_x/\delta_y=0.4$, 7: $\delta_x/\delta_y=0.6$, 8: $\delta_x/\delta_y=1.0$

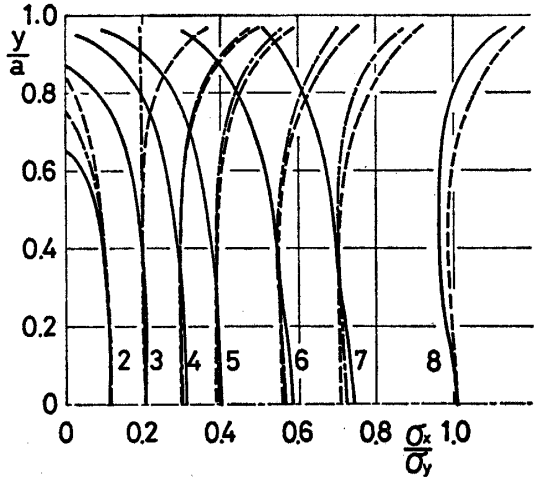

Fig 13–1 Distributions of σ_x/σ_{y0} at $x=a$ for $\mu=0.1$

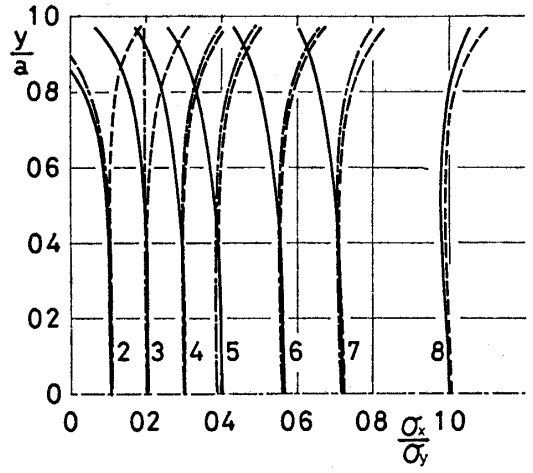

Fig. 13–2 Distributions of σ_x/σ_{y0} at $x=a$ for $\mu=0.05$

—— case A, —·— case B, —··— case C

1: uniaxial, 2: $\delta_x/\delta_y=-0.1$, 3: $\delta_x/\delta_y=0$, 4: $\delta_x/\delta_y=0.1$

5: $\delta_x/\delta_y=0.2$, 6: $\delta_x/\delta_y=0.4$, 7: $\delta_x/\delta_y=0.6$, 8: $\delta_x/\delta_y=1.0$

the coefficients of end friction $\mu=0.1$ and 0.05. From these figures and Fig. 10, it is seen that the distribution of σ_x in the specimen approaches a homogeneous state as the coefficient of end friction decreases.

The ratios of loads in the x-direction to those in the y-direction are shown in Fig. 14 for each path, coefficient of friction and δ_x/δ_y. This ratio is the apparent stress ratio for a given platen displacement. This ratio in case A is lower than that in a perfectly lubricated specimen. In cases B and C, this ratio is higher for $\delta_x/\delta_y>0$ and lower for $\delta_x/\delta_y<0$ than in the case of a perfectly lubricated specimen. This ratio coincides numerically with the area between each curve and the y-axis in Figs. 10–2 and 13. The following is seen from a comparison of Figs. 12 and 13. At $x=a$, σ_x for case A is smaller than that for cases B and C, and at $x=0$, σ_x for case A is larger than that for cases B and C. In another words, in case A, σ_x in the central section ($x=0$) is larger than that calculated from the load, while in cases B and C, σ_x in the central section ($x=0$) is lower than that calculated from the load.

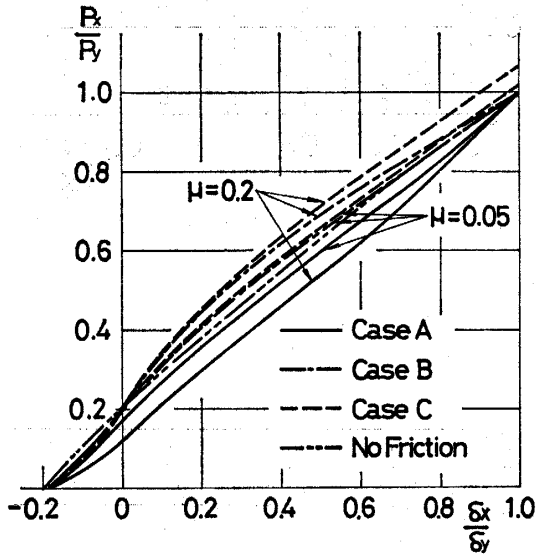

Fig. 14 Px/Py for various loading paths, $\mu,\delta_x/\delta_y$

4. Concluding remarks

The following points may be concluded from the results. They indicate numerous suggestions which might be useful in multiaxial compression tests with steel platens.

(1) Especially in case A, σ_y is large at the corners and small near the point $y=0$ and $x=a$. This tendency is large for a specimen with a large coefficient of end friction.

(2) In case A, a specimen with a large coefficient of end friction tends toward a state of partial loading with slight platen displacement after the apparent isotropic compression state. In cases B and C, the specimen is in the state of partial

loading only for small δ_x/δ_y.

(3) In case A, the apparent σ_x is larger than that at $x=0$, while in cases B and C, it is smaller than that at $x=0$. This difference between the apparent and real distributions of σ_x becomes smaller as the coefficient of end friction decreases.

(4) The deviation of stresses in a specimen from those in a perfectly lubricated specimen is almost proportional to the coefficient of end friction between the specimen and the loading platen. For $\mu=0.05$, the stress distributions become almost uniform.

Reference

1) Niwa, Y., S. Kobayashi and K. Nakagawa: The Influence of End Frictions on Stresses in Compressed Specimens, Memo. Faculty of Eng., Kyoto Univ., 31, 1–10 (1969)